

PAPER • OPEN ACCESS

Sub-urban land classification using GF-2 images and support vector machine method

To cite this article: H S Cui 2019 *IOP Conf. Ser.: Earth Environ. Sci.* **351** 012028

View the [article online](#) for updates and enhancements.

You may also like

- [A Method of Particle Swarm Optimized SVM Hyper-spectral Remote Sensing Image Classification](#)
Q J Liu, L H Jing, L M Wang et al.
- [A Comparison Between Support Vector Machine \(SVM\) and Convolutional Neural Network \(CNN\) Models For Hyperspectral Image Classification](#)
Hayder Hasan, Helmi Z.M. Shafri and Mohammed Habshi
- [Detection of Rice Fields in Sleman District using SVM \(Support Vector Machine\) Method](#)
Sulidar Fitri and Novi Nurjanah



ECS
The
Electrochemical
Society
Advancing solid state &
electrochemical science & technology

DISCOVER
how sustainability
intersects with
electrochemistry & solid
state science research

Sub-urban land classification using GF-2 images and support vector machine method

H S Cui

China Academy of Transportation Science, 240 Huixinli Chaoyang District, Beijing, China

Email: cuihuishan@163.com

Abstract. Remote sensing classification is an important part in the process of extracting effective image information and research the foundation of land cover change. While traditional remote sensing image classification methods have some problems on low accuracy and uncertainty, machine learning algorithms are gradually applied to remote sensing classification. In this paper, support vector machines (SVM) method with high training speed and low computation burden is adopted to classify land cover based on GF-2 image, which is the domestic optical remote sensing satellite with high spatial resolution. The results show that: The overall classification accuracy by SVM is achieved 72.59% and the coefficient of Kappa is 0.65. The classification map is highly consistent with the original image, especially higher classification accuracy of cropland and tree. Partial regions were misclassified as shadow that didn't reflect the real land objects. As a whole, there is favorable classification quality using SVM method and GF-2 multispectral bands.

1. Introduction

Land cover has an important impact on regional water cycle, environmental quality and biodiversity. Remote sensing data can directly record land cover information of the surface. Remote sensing data have constantly given us valuable information for dynamic change applications such as environmental changes, urban sprawl, land cover change, and so on [1-3]. Appropriate correlation analysis tools can help us better understand their insights and timely map land use with less labor.

Classification based on remote sensing is one of the key techniques of image interpretation. Speed and accurate automatic classification algorithm of remote sensing is the key to dynamic monitoring, evaluation and prediction of environment. Due to the large amount of data and high dimension of remote sensing images, as well as the diversity of spectral characteristics and distribution characteristics of different ground objects, the common classification methods have great limitations. Meanwhile, because of the fragmentation and diversity of urban land classes, it is difficult to obtain relatively sufficient and complete sample sets and prior knowledge. Therefore, the classification of sub-urban land faced with many fuzzy objects through lack of self-learning mechanism of statistical parameter classification method.

Combined with rapid development of information technology, remote sensing data get more and more information. Among many machine learning algorithms, support vector machines (SVM) are known to be one of the most effective classification algorithms. It is a general learning methodology developed on the basis of Statistical Learning Theory (SLT) [4]. Moreover, with the increasing complexity of remote sensing data, support vector machine (SVM) framework has been greatly expanded [5,6]. In recent years, SVM algorithm has been widely used in remote sensing image



classification. It can seek the best compromise between the complexity of the model and the learning ability based on the limited sample information, which can obtain the best generalization ability. It is superior in processing small sample, high dimension and nonlinear remote sensing image. Zhu et al. (2002) based on ASTER sensor data proved high performance on convergence, training speed and classification accuracy using SVM algorithm [7]. Bruzzone et al. (2006) proposed an incremental SVM for semi-supervised classification of remote sensing images. Learning in a small sample is more advantageous [8]. Qian et al. (2015) compared the performance of four machine learning classifiers SVM, normal Bayes (NB), classification and regression tree (CART) and K nearest neighbor (KNN) to classify very high resolution images. The result showed that SVM and NB were superior to CART and KNN, particularly for the most commonly-used SVM classifier [9]. Qiao et al. (2017) used Maximum Likelihood Classifier (MLC) and SVM to classify shadow pixels into different land cover types. The results of SVM were verified and find to be consistent with the ground truth values [10]. Zhang et al. (2018) employed SVM algorithm to classify impervious surfaces based on temporal characteristics by seasonal times-series remote sensing imagery. It could accurately map seasonal urban surface dynamics [11].

The rapid development of high-resolution sensor technology provides more accurate location and higher recognition rate of ground objects for remote sensing survey of urban land, thus expanding the depth and breadth of application of remote sensing information. With the development of economy and urbanization, a new special interspace generated in this zone, which was the urban-rural ecotone. Therefore, sub-urban land classification has received widespread attention from high-resolution satellite images. As a high-resolution civil optical remote sensing satellite developed in China, GF-2 satellite effectively improves the comprehensive observation efficiency of China's satellites. Based on SVM algorithm, this paper selects experimental samples for training and classifies GF-2 images into ground objects. The results show that this method has high classification accuracy and spatial stability.

2. Data and methods

2.1. Study area

The study area is located in Henan Province, China (Figure 1). Typical objects in the area include building, road, tree, grass and cropland. It has a warm temperate and sub-humid monsoon climate with abundant thermal resources and abundant sunshine. It is dry and sandy in spring, hot and rainy in summer, sunny in autumn and cold and rainy in winter. The average annual temperate is 15 °C, the average annual precipitation of 700 mm.

2.2. Data sources and pre-processing

GF-2 data is the Chinese civilian optical remote sensing satellite with a resolution superior to 1m and equipped with two high resolution scanners, 1 m panchromatic and 4 m multispectral, respectively. GF-2 satellite was successfully launched on August 19, 2014 [12]. The main users are land resources, urban-rural development and forestry. Detailed payload parameters are showed in Table 1.

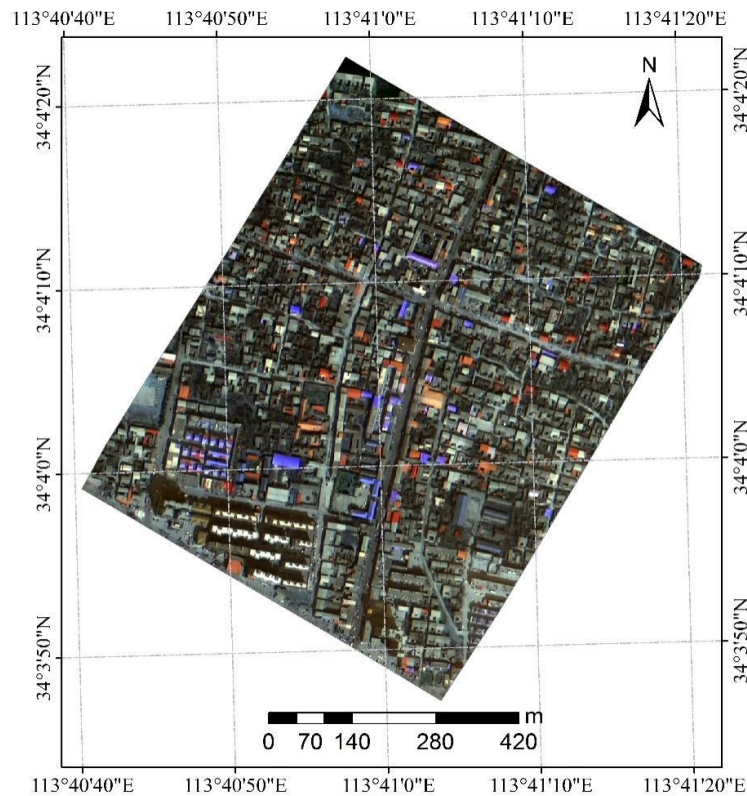


Figure 1. True colour image of study area with GF-2 (R-red, G-green, B-blue; Spatial resolution 1m).

Table 1. Payload parameters of GF-2 satellite.

Spacecraft Payload	Bands	Spectral range (μm)	Spatial resolution (m)	Swath width (km)	Scroll angle ($^{\circ}$)	Revisit interval (days)
Panchromatic camera	1	0.45-0.90	1	45 (2 cameras)	± 35	5
	2	0.45-0.52	4			
Multispectral camera	3	0.52-0.59				
	4	0.63-0.69				
	5	0.77-0.89				

GF-2 data was acquired on 16 February 2017 containing both panchromatic and multispectral bands. The pre-processing of GF images included radiation calibration, atmospheric correction, orthorectification and data fusion. Because electromagnetic wave is affected by the solar position, angle conditions of the sensor and atmospheric conditions in the process of atmospheric transmission and sensor measurement, the target radiation amount measured by the sensor is inconsistent with the actual radiation amount of ground objects. So the radiation distortion of remote sensing image not only reduced the image quality, but also affected the application of image analysis. Radiometric calibration was the process of eliminating radiation distortion in remote sensing image. Atmospheric correction was performed using the Fast Line-of-sight Atmospheric Analysis of Spectral Hypercubes (FLAASH) module based on the improved MODTRAN4+ model. The atmospheric model was set as the mid-latitude winter model. The aerosol type was set to urban type. Atmospheric visibility was set at 40 km, and the average altitude was 200 m. The absolute radiation calibration coefficient and spectral

response function were published by China Centre for Resources Satellite Data and Application. The digital number (DN) of the original image was converted to spectral reflectance value. Then, the panchromatic and multispectral bands were geometrically corrected using the rational polynomial coefficient (RPC) correction module based on digital elevation mode (DEM). The total error of geometric correction and single control point error are controlled within 1 pixels. In addition, the Gram-Schmidt Pan-Sharpener model was used to translate and sharpen the multi-spectral bands and panchromatic bands to obtain very high-resolution (VHR) multi-spectral images with a spatial resolution of 1 m. Image element resampling is performed by cubic convolution algorithm. Meanwhile, the normalized difference vegetation index (NDVI) was one of the best indicators of vegetation growth state and calculated by the VHR multispectral images. The calculation formula is as follows:

$$NDVI = \frac{R_{NIR} - R_{RED}}{R_{NIR} + R_{RED}} \quad (1)$$

where R_{NIR} and R_{RED} represent the reflectance value with the near-infrared band and the red band of GF-2 data, respectively.

Then, VHR multispectral image and NDVI composed into one image data. The above processes were implemented by ENVI software.

2.3. Classification method

Classification method uses SVM [13], which is a supervised classification method based on a set of theoretical machine learning algorithms. We operated the SVM analysis by the independent training data, which was the important step. SVM linear classification initially separates the classes based on a decision surface called the optimal hyper-plane, which maximizes the margin between the classes, and the data points closest to the hyper-plane are called support vectors. Hence, SVM identifies support vectors that have a greater ability to differentiate between classes, thereby constructing a classifier that maximizes the separation between classes and classes. In SVM nonlinear classification, the sample is projected into a high-dimensional linear space based on a non-linear mapping algorithm, in which the optimal hyper-plane is generated. The classification process is simple and based on the kernel function that replaces inner product of the feature space, in which linear methods may be applied. Common kernel functions include linear kernel, polynomial kernel, radial basis kernel and S-shaped kernel [14].

2.4. Sampling data and accuracy assessment

Six classes were selected for the purposes of this comparison study: building, road, tree, grass, cropland and shadow. A random sample of image pixels within the six land cover types was performed. A total of 9041 image pixels were selected on Google earth images with high spatial resolution. 70% of the samples are training data of SVM algorithm, and another 30% are test data of accuracy evaluation (Figure 2). Confusion matrix is used to evaluate the accuracy of classification results. Kappa coefficient, total accuracy, user's accuracy and producer's accuracy are calculated for entire dataset and each class.

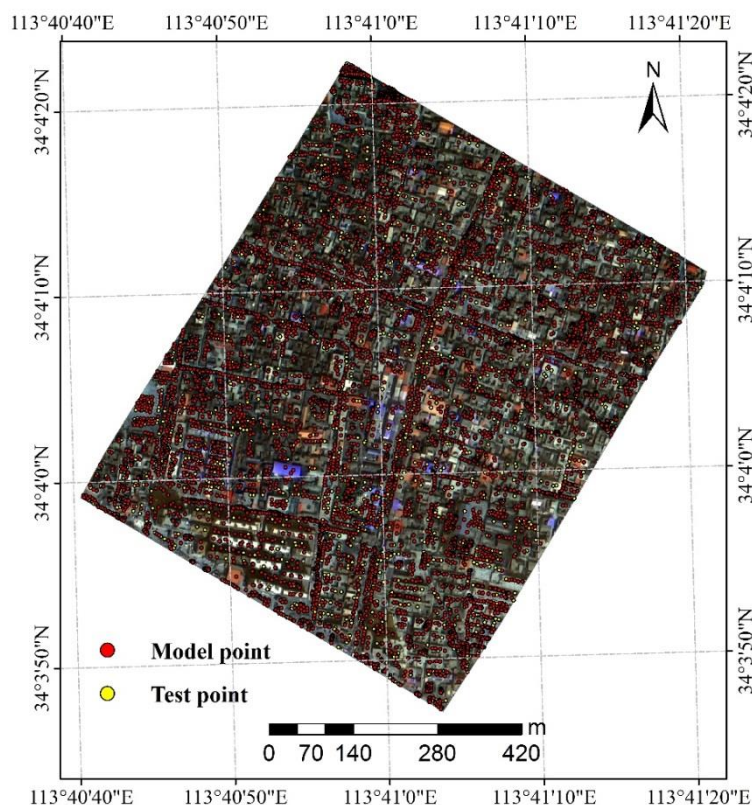


Figure 2. The distribution of training data and testing data.

3. Data and methods

3.1. Results of SVM classification

The SVM classification process is based on a kernel function, we use the radial basis function (RBF) kernel because it has proved more effective for many classification applications [15-18]. The penalty parameter was set to 1000, and the other parameters were based on the default after several tests. The image resulting from the SVM classification was shown in Figure 3. Six different classes were established: building, road, tree, grass, cropland and shadow. Based on the classification results of confusion matrix, the total accuracies were 72.59%, Kappa coefficient were 0.65. Table 2 showed that the classification of cropland and shadow were best. The producer's accuracy and user's accuracy were greater than 85%. The classification accuracies of tree were secondary, producer's accuracy and user's accuracy were 78.71% and 71.29%, respectively. Building was low, producer's accuracy and user's accuracy were 69.86% and 69.77%, respectively. The classification accuracy of grass and road was the lowest. User's accuracy was both less than 70%, producer's accuracy of grass and road was only 44.65% and 62.19%.

GF-2 image had better classification performance of cropland and tree when extracting vegetation information. GF-2 images contain near-infrared band and red band, which are sensitive to vegetation. While grass and cropland are non-dominant classes in this area, cropland class was precisely identified as higher than grass class. This could be caused by textures of cropland obviously described than grass. It showed that GF-2 performs extremely well at distinguishing between cropland class and other classes.

However, extracting road and building information is not ideal, they were misclassified to some extent, mainly due to the similarity of the spectrum. Future work will add multi-sources or features to distinguished road and building. For example, normalized digital surface model (nDSM) derived from LiDAR data will greatly classify building and road by height feature.

On general visual inspection, the classification results produced a speckled “salt-and-pepper” effect, because adjacent pixels are lacking comprehensive analysis. Further studies should compare object-based SVM algorithm or other machine learning methods to created visually acceptable depictions of the broad land cover classes present within the study area.

Table 2. Confusion matrices based on test data.

Class	Building_t	Cropland_t	Grass_t	Road_t	Shadow_t	Tree_t	Total	User's accuracy
Building_m	510	0	1	187	3	30	731	69.77%
Cropland_m	0	45	0	0	0	0	45	100.00%
Grass_m	14	0	96	2	0	40	152	63.16%
Road_m	156	0	8	380	1	30	575	66.09%
Shadow_m	15	0	2	4	412	39	472	87.29%
Tree_m	35	0	108	38	26	514	721	71.29%
Total	730	45	215	611	442	653	2696	
Producer's accuracy	69.86%	100.00%	44.65%	62.19%	93.21%	78.71%		

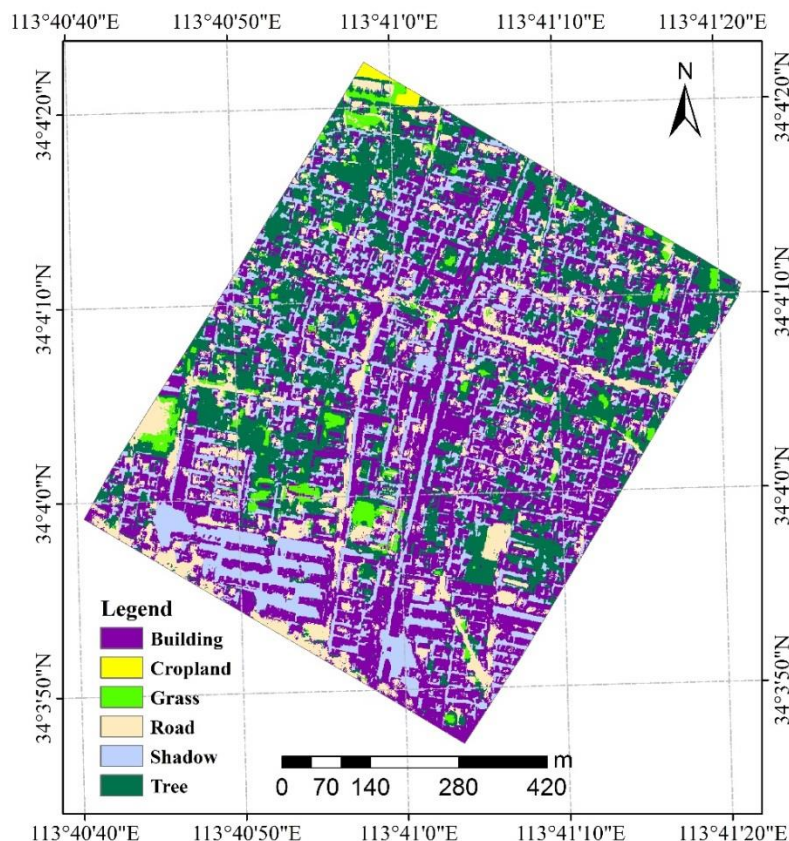


Figure 3. Land cover mapping based on the SVM algorithm.

3.2. Area distribution of sub-urban lands

Areas of different land cover were calculated with classification results (Table 3). Area of building was 221446 m² accounting for 7.04% of region, which was the largest area. Area of tree was less than building and accounted for 25.81% of region. Because of the height of building in the city, urban land

generated a lot of shadow area in direct sunlight. Area of shadow was 129130 m², accounting for 21.60% of region. The shadow classification included road, tree and grass. The road area was 75890 m², accounting for 12.7% of region. Grass land area was 15417 m² accounting for 2.58%. The area of cropland was least than other sub-urban lands, only accounting for 0.27%.

Based on VHR multispectral images there is a shadow effect of classification results in our experiment area. This finding was consistent with other studies [19]. The work presented will further be improved by incorporating LiDAR for the land cover classification. LiDAR could provide elevation information and eliminate the shadow problem.

Table 3. Area and proportion of sub-urban land classification.

Classification	Area (m ²)	Percent (%)
Building	221446	37.04
Cropland	1588	0.27
Grass	15417	2.58
Road	75890	12.70
Shadow	129130	21.60
Tree	154315	25.81

Overall, compared with other VHR optical satellite sensors, GF-2 data can provide better classification mapping accuracy in sub-urban environments. Its advantage had ability to distinguish spectral differences between land covers, especially between shadow and tree. The classification accuracy of urban land cover was estimated based on QuickBird image, with a total accuracy of 69.12% and a kappa coefficient of 0.62 [20]. Hamedianfar et al. (2014) achieved the classification results using WorldView-2 imagery and the two machine learning methods, yielding overall accuracies of 72.46% and 75.69%, respectively [21].

4. Conclusion

In this paper, we verified the potential classification accuracy of GF-2 satellite data, and found that the classification mapping accuracy of gf-2 multi-spectral data in sub-urban zone was relatively good. SVM machine learning performed better classification in this study zone, and the total accuracy was 72.59%, Kappa coefficient was 0.65. Cropland and shadow were the best classification accuracy, followed by tree, building, and grass, road. The producer's accuracy of cropland and shadow were more than 93%, and the user's accuracy was more than 87%. GF-2 image had good performance in extracting vegetation information, especially in cropland and tree. However, distinguishing between building and road using GF-2 multi-spectral band and NDVI is difficult, they were misclassified. In general, region-based classifiers can improve classification accuracy. We will further study more accurate classification methods on sub-urban land classification in the future.

Acknowledgments

We are grateful for support from Central Public Welfare Research Project "Ecological Impact Assessment of Road Network Construction in Temperate Grassland Area", (Project No. 20160607).

References

- [1] Tucker C J, Townshend J R G and Goff T E 1985 African landcover classification using satellite data *Science* **227** 369-75
- [2] Dewan A M and Yamaguchi Y 2009 Land use and land cover change in Greater Dhaka, Bangladesh: using remote sensing to promote sustainable urbanization *Appl. Geography*. **29** 390-401
- [3] Tanaka S and Nishii R 2009 Nonlinear regression models to identify functional forms of deforestation in East Asia *IEEE Trans. Geosci. Remote Sens.* **47** 2617-26

- [4] Cortes C and Vapnik V 1995 Support-vector networks *Mach. Learn.* **20** 273-97
- [5] Crammer K and Singer Y 2001 On the algorithmic implementation of multiclass kernel-based vector machines *J. Mach. Learn. Res.* **2** 265-92
- [6] Konstantinos K, Grigorios T, Michalis Z and Panagiotis T 2015 Deep learning for multi-label land cover classification *Proc. SPIE, Image and Signal Process. Remote Sens.* 9643. doi: 10.1117/12.2195082
- [7] Zhu G B and Blumberg D G 2002 Classification using ASTER data and svm algorithms: the case study of Beer Sheva, Israel *Remote Sens. Environ.* **80** 233-40
- [8] Bruzzone L, Chi M and Marconcini M 2006 A novel transductive svm for semi-supervised classification of remote-sensing images *IEEE Trans. Geosci. Remote Sens.* **44** 3363-73
- [9] Qian Y G, Zhou W Q, Yan J L, Li W F and Han L J 2015 Comparing machine learning classifiers for object-based land cover classification using very high resolution imagery *Remote Sens.* **7** 153-68
- [10] Qiao X J, Yuan D S and Li H 2017 Urban shadow detection and classification using hyperspectral image *J. Indian Soc. Remote Sens.* **45** 945-952
- [11] Zhang L, Zhang M and Yao Y B 2018 Mapping seasonal impervious surface dynamics in Wuhan urban agglomeration, China from 2000 to 2016 *Int. J. Appl. Earth Obs. Geoinf.* **70** 51-61
- [12] Wu Q, Zhong R F, Zhao W J, Song K and Du L M 2019 Land-cover classification using GF-2 images and airborne lidar data based on random forest *Int. J. Remote Sens.* **40** 2410-26
- [13] Chang C C and Lin C J 2007 LIBSVM: A library for support vector machines *ACM Trans. Intell. Syst. Technol.* **2** 389-96
- [14] Wu Q, Zhong R F, Zhao W J, Fu H, and Song K 2017 A comparison of pixel-based decision tree and object-based support vector machine methods for land-cover classification based on aerial images and airborne lidar data *Int. J. Remote Sens.* **38** 7176-95
- [15] Kavitha K, Arivazhagan S and Sangeetha I K 2015 Hyperspectral image classification using support vector machine in Ridgelet Domain *Natl. Acad. Sci. Lett.-India* **38** 475-78
- [16] Cho G S, Gantulga N and Choi Y W 2017 A comparative study on multi-class SVM and kernel function for land cover classification in a KOMPSAT-2 image *KSCE J. Civ. Eng.* **21** 1894-904
- [17] Dasari K and Lokam A 2018 Exploring the capability of compact polarimetry (hybrid pol) c band RISAT-1 data for land cover classification *IEEE Access* **6** 57981-93
- [18] Esmael A A, Santos J A D and Torres R D 2018 On the ensemble of multiscale object-based classifiers for aerial images: a comparative study *Multimed. Tools Appl.* **77** 24565-92
- [19] Yan W Y, Shaker A and El-Ashmawy N 2015 Urban land cover classification using airborne lidar data: a review *Remote Sens. Environ.* **158** 295-310
- [20] Chen Y, Su W, Li J and Sun Z 2009 Hierarchical object oriented classification using very high resolution imagery and lidar data over urban areas *Adv. Space Res.* **43** 1101-10
- [21] Hamedianfar A, Shafri H Z M, Ahmad N and Ahmad N 2014 Improving detailed rule-based feature extraction of urban areas from worldview-2 image and lidar data *Int. J. Remote Sens.* **35** 1876-99